IC/90/32

INTERNATIONAL CENTRE FOR THEORETICAL PHYSICS

FERMI HYPER-NETTED CHAIN THEORY ON A LATTICE: THE HUBBARD MODEL

X.Q. Wang

S. Fantoni

E. Tosatti

Yu Lu

and

X.Q.G. Wang

INTERNATIONAL ATOMIC ENERGY AGENCY

UNITED NATIONS EDUCATIONAL, SCIENTIFIC AND CULTURAL ORGANIZATION

1990 MIRAMARE - TRIESTE

International Atomic Energy Agency

and

United Nations Educational Scientific and Cultural Organization

INTERNATIONAL CENTRE FOR THEORETICAL PHYSICS

FERMI HYPER–NETTED CHAIN THEORY ON A LATTICE: THE HUBBARD MODEL *

X.Q. Wang

International School for Advanced Studies, Trieste, Italy,

S. Fantoni

Department of Physics and INFN, University of Lecce, Lecce, Italy,

E. Tosatti

International Centre for Theoretical Physics, Trieste, Italy

and

International School for Advanced Studies, Trieste, Italy,

Yu Lu

International Centre for Theoretical Physics, Trieste, Italy

and

Institute of Theoretical Physics, Academia Sinica, Beijing, People's Republic of China

and

X.Q.G. Wang **

International School for Advanced Studies, Trieste, Italy.

MIRAMARE – TRIESTE

February 1990

* To be published in **Recent Progress in Many Body Theory**, Vol.2, Y. Avishai et al. eds., Plenum Press, London.

** In the future papers, X.Q.G. Wang always represents Xiaoqun Wang or Wang Xiaoqun as distinct from X.Q. Wang, representing Xiaoqian Wang, a different person.

ABSTRACT

We review a new lattice version of Fermi Hyper–Netted Chain method for the study of strongly interacting electrons. The ordinary paramagnetic and the spin density wave functions have been correlated with Jastrow–type and $e-d$ correlations, and the corresponding FHNC equations for the pair distribution function, the one body density matrix and the staggered magnetization are discussed. Results for the $1\,D$ chain and $2\,D$ square lattice models are presented and compared with the available results obtained within Quantum Monte Carlo, variational Monte Carlo and exact diagonalization of a 4×4 Hubbard cluster. Particularly interesting are the strong effects of $e-d$ correlations on E/Nt and on the momentum distribution as well as antiferromagnetic behavior away from half filling found in our FHNC calculations in agreement with other studies.

1 Introduction

The quantitative understanding of correlation effects in strongly interacting system is a challenging issue in Many-Body physics. In most cases of interest such effects can hardly be handled by means of conventional perturbation theories *built upon independent particle basis functions*. Most notable are stochastic methods, such as Green Function Monte Carlo[1], and theories using correlated basis functions (CBF)[2] which have allowed for very accurate *ab initio* calculations in systems like liquid helium, high density neutron matter and nuclear matter[3].

In solid state physics much effort has been devoted to study the behavior of electrons in narrow band systems, their localization property and the strong correlation effects. The Hubbard hamiltonian[4,5] given by

$$H = -t \sum_{<i,j>,\sigma} c^{\dagger}_{i\sigma} c_{j\sigma} + U \sum_{i} n_{i\uparrow} n_{i\downarrow}, \qquad (1)$$

where i, j are sites of a D-dimensional lattice, t is the hopping energy, and U is the on-site repulsion, is a well-known prototype model which incorporates the main features of such systems, namely itinerant magnetism and metal-insulator transition[6]. More recently, interest in the Hubbard model has been revived by Anderson's suggestion[7] that non-Fermi liquid behavior away from $\frac{1}{2}$ filling might be at the origin of high T_c superconductivity.

In $D = 1$ dimension it has been exactly solved by Lieb and Wu[8], and recently developed methods of numerical solution[9,10] as well as variational approaches[11-13] have been widely applied to the cases with D = 1,2,3. Similar attention has also been devoted to related spin- $\frac{1}{2}$ antiferromagnetic Heisenberg and quantum nonlinear σ models[14]. In spite of the enormous proportions acquired by the literature, the deep physics of this model is still open to discussion.

The variational approaches have been very useful to understand the role played by certain type of correlations, like for instance the on-site (Gutzwiller)

correlations and those between empty and doubly occupied sites($e-d$ correlations)[13,15]. The variational ground state is taken of the form

$$|\Psi_0> = G|\Phi_0>, \qquad (2)$$

where $|\Phi_0>$ is a reference state which can be expressed as a Slater determinant of single particle states and G is a correlations operator building into $|\Phi_0>$ those correlation which lower the energy upperbound.

Typical reference states considered so far are the ordinary paramagnetic state $|\Phi_P>$, the BCS state $|\Phi_{BCS}>$ and the spin density wave state $|\Phi_{SDW}>$. In contrast to $|\Phi_P>$ which has a Fermi surface, both $|\Phi_{BCS}>$ and $|\Phi_{SDW}>$ do not show Fermi liquid character and have long range order.

The correlation operator which has been mostly used has the Jastrow form:

$$G_J = \prod_{ij} f_J(r_{ij}) \qquad (3)$$

which, in the case of on-site correlations $f(r_{ij})$, has been commonly denoted as Gutzwiller projection operator. In fact, finite range two-body correlations do not lead[13] to a significant lowering of the energy. However, the optimization of the function $f(r_{ij})$ is expected to be important for a realistic evaluation of quantities of interest like the momentum distribution and the single particle spectrum[16]. Other type of correlations as the spin-dependent correlations or the four-body correlations simulating the $e-d$ correlation have been found to play an important role.

Recently[13], the Fermi Hyper-Netted Chain (FHNC) scheme has been implemented for the Hubbard discrete lattice model. The results for the $D = 1$ case are in very good agreement with the available variational Monte Carlo estimates. The FHNC scheme has a few advantages over the Monte Carlo method: (i) it can be done at the outset for the thermodynamic limit, *avoiding* the problems concerning the finite size effects which can be serious in $D = 2$, 3 dimensions; (ii) it is very flexible as far as the possible choice of correlation operator is

concerned: for instance, finite range (and also long range) correlations do not constitute a serious problem; similarly three-, four-body correlations or spin-dependent correlations can be handled. Actually, this has already been done in nuclear matter[17], liquid helium[18] and, more recently, in $1D$ Hubbard model[13], (iii) the solution of hamiltonians which are more realistic than (1) for describing the copper-oxide materials, like the two-band model hamiltonian[19] are certainly at the reach of the method; (iv) it allows for applying the full *machinery* of CBF theory[20,21] to go beyond the variational estimates, which may be *crucial* to determine the phase disgram of the system as a function of the filling factor and the coupling constant U/t.

On the other hand, the FHNC diagrammatic expansion at present cannot be expressed in a fully closed form, which makes this approach intrinsically approximate. Higher levels of approximations (FHNC/n), although formally doable, require increasing amount of analytical work. By contrast, the *accuracy* of stochastic methods is in practice limited only by the computer capabilities.

It is gratifying that already at the lowest order approximation, the FHNC/0, a reasonable agreement with the available Monte Carlo results is obtained for the $1D$ Hubbard model *for* $U/t \leq 8$.

In this contribution we discuss the FHNC scheme to calculate the expectation value of the hamiltonian (1) with trial wave function (2) with G of the Jastrow form G_J and $\Phi_0 = \Phi_{SDW}$. The SDW state is a band insulator at any filling with the Fermi surface being destroyed by single particle Bragg scattering. It has an antiferromagnetic long range order (AFLRO) that is maintained in the correlated Ψ_{SDW}. It has recently been reconsidered by Schrieffer *et al*[22] in a study of high T_c superconductivity. In fact, neutron[23] and Raman[24] scattering experiments on superconducting materials have shown that finite range antiferromagnetic correlations exist in superconducting phase and that AFLRO occurs in the phase diagram near the superconducting phase. Therefore, it is interesting to calculate at T=0 the staggered magnetization of the Hubbard

hamiltonian for a Jastrow correlated model as a function of U/t and the filling factor ν. The proposed method also allows for evaluating the momentum distribution, the charge and spin structure functions and the staggered magnetization of the model. Moreover, the same scheme can be used to calculate the diagonal matrix elements of (1) between correlated basis SDW states given by

$$\Psi_{SDW}(p_1,...,p_n;h_1,...,h_n) = G_J\Phi_{SDW}(p_1,...,p_n;h_1,...,h_n) \qquad (4)$$

where $\Phi_{SDW}(p_1,...,p_n;h_1,...,h_n)$ is the Slater determinant of SDW single particle states having the n-particle states p_1, ..., p_n and the n hole-states h_1, ..., h_n. This calculation provides the variational estimate of the single particle spectrum which is a key ingredient for future CBF perturbative calculations.

The FHNC scheme to be used with the Jastrow correlated SDW model is discussed in section 2. The last section is devoted to a discussion of the results obtained within the FHNC approach and those concerning the magnetic properties of the Jastrow correlated models.

2 Correlated spin-density wave theory

The reference state Φ_{SDW} is a Slater determinant of single particle wave functions given by[22]

$$\psi^{<}_{\mathbf{k}\sigma}(r_i) = (u(\mathbf{k})e^{i\mathbf{k}\cdot\mathbf{r}_i} + \hat{\sigma}_z(i)v(\mathbf{k})e^{i(\mathbf{k}+\mathbf{Q})\cdot\mathbf{r}_i})\xi_\sigma(i) \qquad (5)$$

for $\mathbf{k}$ imbedded in the Fermi sea S_F corresponding to the half-filling case, characterized by $\cos k_x a\ (+\cos k_y a) \geq 0$ in $1D$ ($2D$ square lattice(SQL)), and

$$\psi^{>}_{\mathbf{k}\sigma}(r_i) = (u(\mathbf{k})e^{i\mathbf{k}\cdot\mathbf{r}_i} - \hat{\sigma}_z(i)v(\mathbf{k})e^{i(\mathbf{k}+\mathbf{Q})\cdot\mathbf{r}_i})\xi_\sigma(i) \qquad (6)$$

for $\cos k_x a\ (+\cos k_y a) \leq 0$. ξ_σ is the spin eigenfunction, and $\mathbf{Q}$ is the wavevector characterizing the extra-periodicity due to the antiferromagnetic ordering. In principle, $\mathbf{Q}$ might depend on the filling factor and should be kept as a variational

parameter. Here we consider a single two-sublattice antiferromagnetic structure, which implies $\mathbf{Q}$ is defined by the condition $e^{i\mathbf{Q}\cdot\mathbf{r}_i} = -1$ for all translations t which transform a sublattice into the other. Thus $\mathbf{Q}$ is $\frac{\pi}{a}$ for $1D$ and $(\frac{\pi}{a},\frac{\pi}{a})$ for $2D$-SQL.

The orthonormalization conditions $u^2(k) + v^2(k) = 1$, $u(|\mathbf{k} \pm \mathbf{Q}|) = v(k)$ and $v(|\mathbf{k} \pm \mathbf{Q}|) = u(k)$ constrain the functions $u(k)$ and $v(k)$ which can be taken of the form

$$u(k) = (\frac{1}{2}(1 + \frac{\epsilon(k)}{E_0(k)}))^{\frac{1}{2}}, \tag{7}$$

$$E_0(k) = (\epsilon^2(k) + \Delta^2)^{\frac{1}{2}}, \tag{8}$$

where $\epsilon(k) = -2t\cos k_x a$ for $1D$ and $\epsilon(k) = -2t\,(\cos k_x a + \cos k_y a)$ for $2D$-SQL. The uncorrelated single particle spectrum is given by $E_0(k)$ for $k < k_F(\nu = \frac{1}{2})$ and $-E_0(k)$ for $k > k_F(\nu = \frac{1}{2})$. The gap parameter Δ at $k = k_F(\nu = \frac{1}{2})$ is given by[29]

$$\Delta = Um/2, \tag{9}$$

where m is the spin polarization per particle in the z-direction. In the present correlated model Δ is taken as a variational parameter and the relation (9) is no longer valid. The ordinary paramagnetic correlated ground state is a special case of this function, with $\Delta = 0$.

The expectation value of the hamiltonian is given by[13]

$$E_0 = < H > /N = -2t\rho n(\mathbf{r}_a) + U\rho^2 g(0)/2, \tag{10}$$

where N are the lattice points separated by a, $\rho = A/N = 2\nu$ is the density and $\mathbf{r}_a = a$ in $1D$ and (a,a) in $2D$-SQL. The functions $g(\mathbf{r}_{ij})$ and $n(\mathbf{r}_{ij})$ are the pair distribution function and the one-body density matrix, respectively. In the uncorrelated model ($f = 1$) one has $g(0) = 1 - \frac{1}{2}\,l_u^2(0) - \frac{1}{2}\,l_v^2(0)$ and $n(a) = l_n(a)$ (see eqs. (17),(18))and $E_0 = 0$ in both limits $U/t \to 0$ and $U/t \to \infty$.

2.1 The FHNC scheme for $g(\mathbf{r}_{ij})$

The pair distribution function is calculated by first expressing G_J^2 as a sum of cluster terms[25]:

$$G_J^2 = \prod_{i<j} f^2(\mathbf{r}_{ij}) = X_2(\mathbf{r}_1,\mathbf{r}_2) + \sum_{i>2} X_3(\mathbf{r}_1,\mathbf{r}_2,\mathbf{r}_i) + ..., \tag{11}$$

$$X_2(\mathbf{r}_1,\mathbf{r}_2) = f^2(r_{12}) \tag{12}$$

$$X_3(\mathbf{r}_1,\mathbf{r}_2,\mathbf{r}_i) = f^2(r_{12})(h(\mathbf{r}_{1i}) + h(\mathbf{r}_{2i}) + h(\mathbf{r}_{1i})h(\mathbf{r}_{2i})), \tag{13}$$

where the dynamical correlation $h(\mathbf{r}_{ij}) = f^2(\mathbf{r}_{ij}) - 1$. It results that $g(\mathbf{r}_{ij})$ is given by

$$g(\mathbf{r}_{12}) = \frac{1}{\aleph}\rho^2 \sum_p \frac{\rho^p}{(p-2)!} \sum_{\mathbf{r}_3,...,\mathbf{r}_p} X_p(\mathbf{r}_1,...,\mathbf{r}_p)\Delta_p(\mathbf{r}-1,...,\mathbf{r}_p), \tag{14}$$

where Δ_p are the p-body uncorrelated distribution functions:

$$\Delta_p(\mathbf{r}_1,...,\mathbf{r}_p) = \frac{A(A-1)(A-p+1)}{\rho^p} \frac{\sum_{\mathbf{r}_{p+1}...\mathbf{r}_N} |\Phi_{SDW}|^2}{\sum_{\mathbf{r}_1...\mathbf{r}_N} |\Phi_{SDW}|^2}, \tag{15}$$

and $\aleph = < \Psi_{SDW}|\Psi_{SDW} >$ is the normalization. As in the ordinary paramagnetic case, Δ_p can be expressed in terms of the uncorrelated density matrix:

$$\begin{aligned}
\hat{\rho}(1,2) &= \frac{1}{N}\sum_{\mathbf{k},\sigma} \phi^*_{\mathbf{k}\sigma}(1)\phi_{\mathbf{k}\sigma}(2) \\
&= \frac{1}{2}\sum_{\sigma} \xi^*_\sigma(1)\xi_\sigma(2)[l_u(\mathbf{r}_{12}) + e^{i\mathbf{Q}\cdot\mathbf{r}_{12}} l_v(\mathbf{r}_{12}) sign(\sigma)] \\
&= \frac{1}{2}\sum_{\sigma} \xi^*_\sigma(1)\xi_\sigma(2)\hat{\rho}_\sigma(\mathbf{r}_{12}),
\end{aligned} \tag{16}$$

where $sign(\sigma)$ takes either $+1$ or -1 corresponding to $\xi_\sigma = \uparrow$ or $\downarrow$, and

$$l_u(\mathbf{r}_{12}) = \frac{2}{N}\sum_{\mathbf{k}\in F_1} \{(u^2(\mathbf{k})e^{-i\mathbf{k}\cdot\mathbf{r}_{12}} + v^2(\mathbf{k})e^{-i(\mathbf{k}+\mathbf{Q})\cdot\mathbf{r}_{12}}\}, \tag{17}$$

$$l_v(\mathbf{r}_{12}) = \frac{2}{N}\sum_{\mathbf{k}\in F_1} u(\mathbf{k})v(\mathbf{k})e^{-i\mathbf{k}\cdot\mathbf{r}_{12}}(1 + \cos(\mathbf{Q}\cdot\mathbf{r}_{12})). \tag{18}$$

The density matrices $\hat{\rho}(i,j)$ appear in Δ_p in the form of closed separate loops, each with a factor $-(-1/2\rho)^m$, with m being the number of loop-points. The

loops with $m > 2$ have an extra factor 2, since they are originated by two different cyclic permutations. Since the dynamical correlations are spin-independent they do not affect the spin traces and one has

$$\Delta_P = 1 - (\frac{1}{2\rho})^2 \sum_{i<j} \sum_{\sigma_i \sigma_j} \hat{\rho}(i,j)\hat{\rho}(j,i) + 2(\frac{1}{2\rho})^3 \sum_{i<j<k} \sum_{\sigma_i \sigma_j \sigma_k} \hat{\rho}(i,k)\hat{\rho}(k,j)\hat{\rho}(j,i) + ... \quad (19)$$

It follows that $\rho^2 \aleph g(r_{12})$ is given by a series of cluster terms, each being a product of dynamical correlations and exchange operators, so that each particle variable of the cluster, except for $\mathbf{r}_1$ and $\mathbf{r}_2$ is argument of at least one dynamical correlation.

In eq. (14) for every p there are $(p-2)!/S$ cluster terms which differ only in the way of labelling the $p-2$ indices (S is the symmetry number). One can then remove the $(p-2)!$ factor in eq.(14) and sum over the topologically distinct cluster terms.

The normalization $\aleph$ has obviously the same structure as $\rho^2 \aleph g(r_{12})$. As a consequence (being the sum over p extended to infinity), $\rho^2 \aleph g(r_{12})$ can be factorized in a sum of linked cluster terms containing $f^2(r_{ij})$, times $\aleph$, with the result

$$g(r_{12}) = \frac{1}{\rho^2} f^2(r_{12}) \sum_p \rho^p \sum_{\mathbf{r}_3,...,\mathbf{r}_p} L_p(\mathbf{r}_3,...,\mathbf{r}_p), \quad (20)$$

where L_p represents the sum of all linked, topologically distinct cluster terms having the (external) variables $\mathbf{r}_1, \mathbf{r}_2$ and other $(p-2)$ internal particle variables.

Since $\hat{\rho}(i,j)$ satisfy the convolution property $\sum_{\mathbf{r}_k \sigma_k} \hat{\rho}(i,k)\ \hat{\rho}(k,j) = \hat{\rho}(i,j)$, then all the separable cluster terms of $g(\mathbf{r}_{12})$ cancel each other and one is finally left with the sum over the topologically distinct irreducible cluster terms I_p:

$$g(r_{12}) = \frac{1}{\rho^2} f^2(r_{12}) \sum_p \rho^p \sum_{\mathbf{r}_3,...\mathbf{r}_p} I_p(\mathbf{r}_1,...\mathbf{r}_p). \quad (21)$$

A few examples of cluster diagrams representing I_p are reported on Fig. 1.

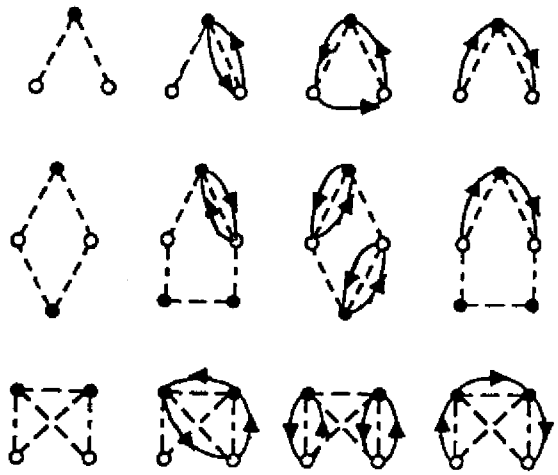

Fig.1 Examples of cluster diagrams contributing to $g(\mathbf{r}_{ij})$. The open dots represent the external variables i and j, whereas the solid dots denote internal variables, upon which summation is implied. Dashed and oriented solid lines represent dynamical correlation $h(r_{mn})$ and exchange operator $\hat{\rho}(m,n)$, respectively. The diagrams in the first row are chain (nodal), those in the second row are composite and the diagrams in the bottom row are elementary. Diagrams in the first column are of the $dd-$type; $de-$, $ee-$and $cc-$ diagrams are displayed in the subsequent columns.

The FHNC scheme to calculate $g(\mathbf{r}_{12})$ is very similar to that needed for the ordinary paramagnetic case[13]. The chain equations for N_{dd}, N_{de} and N_{ee} are exactly the same as in Ref. 13 and therefore will not be reported here. On the contrary, because of the two-component structure of $\hat{\rho}(i,j)$ and because of the presence of the phase factor $e^{i\mathbf{Q}\cdot\mathbf{r}_{ij}}$, the calculation of the (cyclic-cyclic) chain diagrams N_{cc} and of the composite diagrams X_{cc} and X_{ce} requires some more discussion. It is useful to represent the cyclic diagrams with two-component

vector quantities as:

$$\begin{aligned}\hat{Z}(ij) &\equiv (Z_u(\mathbf{r}_{ij}), Z_v(\mathbf{r}_{ij})) \\ &= \sum_\sigma \xi^*_\sigma(i)\xi_\sigma(j)\{Z_u(\mathbf{r}_{ij}) + sign(\sigma)e^{i\mathbf{Q}\cdot\mathbf{r}_i} Z_v(\mathbf{r}_{ij})\}. \end{aligned} \quad (22)$$

The components of $\hat{\rho}(ij)$ are given by $l_u(\mathbf{r}_{ij})$ and $l_v(\mathbf{r}_{ij})$, respectively. The convolution integral is defined as

$$\hat{Z}(ij) = (\hat{F}(ik)|\hat{G}(kj)), \quad (23)$$

$$Z_u(\mathbf{r}_{ij}) = \rho\sum_{\mathbf{r}_k}\{F_u(r_{ik})G_u(r_{kj}) + F_v(r_{ik})G_v(r_{kj})\cos(\mathbf{Q}\cdot\mathbf{r}_{ik})\}, \quad (24)$$

$$Z_v(\mathbf{r}_{ij}) = \rho\sum_{\mathbf{r}_k}\{F_v(r_{ik})G_u(r_{kj}) + F_u(r_{ik})G_v(r_{kj})\cos(\mathbf{Q}\cdot\mathbf{r}_{ik})\}. \quad (25)$$

The parallel connection between two vector quantities is a scalar given by:

$$\hat{F}(ij) * \hat{G}(ij) = 2F_u(r_{ij})G_u(r_{ij}) + 2\cos(\mathbf{Q}\cdot\mathbf{r}_{ij})F_v(r_{ij})G_v(r_{ij}), \quad (26)$$

In doing the chain summation one has to keep track of the ordering of the various cc-elements due to the asymmetrical structure of convolution integral (23-25), with the result

$$\begin{aligned}\hat{N}_{cc}(ij) &= (\hat{X}_{cc}(ik) + \hat{N}_{cc}(ik) - \frac{1}{2}\hat{\rho}(ik)|\hat{X}_{cc}(kj) \\ &- \frac{1}{2}(\hat{X}_{cc}(kl)|\hat{\rho}(lj))) - \frac{1}{2}(\hat{X}_{cc}(ik)|\hat{\rho}(kj)). \end{aligned} \quad (27)$$

This equation reduces to the conventional FHNC equation for $N_{cc}(r_{ij})$ when $l_v(r_{ij}) = 0$. The composite diagrams X_{cc} and X_{ee} are summed by

$$\hat{X}_{cc}(ij) = (g_{dd}(\mathbf{r}_{ij}) - 1)(\hat{N}_{cc}(ij) - \frac{1}{2}\hat{\rho}(ij)) + g_{dd}(\mathbf{r}_{ij})\hat{E}_{cc}(ij), \quad (28)$$

$$\begin{aligned}\hat{X}_{ee}(ij) &= g_{dd}(\mathbf{r}_{ij})[N_{ee}(\mathbf{r}_{ij}) + E_{ee}(\mathbf{r}_{ij}) + (N_{de}(\mathbf{r}_{ij}) + E_{de}(\mathbf{r}_{ij}))^2 \\ &- 2(\hat{N}_{cc}(ij) + \hat{E}_{cc}(ij) - \frac{1}{2}\hat{\rho}(ij))^2] - N_{ee}(\mathbf{r}_{ij}), \end{aligned} \quad (29)$$

where $g_{dd}(\mathbf{r}_{ij}) = f^2(r_{ij})\exp\{N_{dd}(\mathbf{r}_{ij}) + E_{dd}(\mathbf{r}_{ij})\}$, and $E_{\alpha\beta}(ij)$ refers to the sum of bridge (elementary) diagrams of the $\alpha\beta$-type.

In terms of the FHNC-quantities the pair distribution function is given by:

$$\begin{aligned}g(\mathbf{r}_{12}) &= 1 + X_{dd}(\mathbf{r}_{12}) + N_{dd}(\mathbf{r}_{12}) + 2X_{de}(\mathbf{r}_{12}) + 2N_{de}(\mathbf{r}_{12}) \\ &+ N_{ee}(\mathbf{r}_{12}) + X_{ee}(\mathbf{r}_{12}), \end{aligned} \quad (30)$$

and the density-density correlation function $S(\mathbf{k}) = < \rho^\dagger_{\mathbf{k}}\rho_{\mathbf{k}} >$, with $\rho_{\mathbf{k}} = \frac{1}{\sqrt{N}}$ $\sum_i exp(i\mathbf{k}\cdot\mathbf{r}_i)$, is obtained from $g(\mathbf{r}_{12})$ by means of the equation

$$S(k) = 1 + \rho\sum_{\mathbf{r}_i}(g(\mathbf{r}_i) - 1)\cos(\mathbf{k}\cdot\mathbf{r}_i). \quad (31)$$

Similarly, the spin-spin correlation function $S_\sigma(\mathbf{k}) = < \rho^\dagger_{\sigma,\mathbf{k}}\rho_{\sigma,\mathbf{k}} >$, with $\rho_{\sigma,\mathbf{k}} =$ $\frac{1}{\sqrt{N}}\sum_i exp(i\mathbf{k}\cdot\mathbf{r}_i)\sigma_z(i)$, is given by

$$\begin{aligned}S_\sigma(\mathbf{k}) &= 1 + \rho\sum_i \cos(\mathbf{k}\cdot\mathbf{r}_i)\{X_{ee}(\mathbf{r}_i) + N_{ee}(\mathbf{r}_i)\} \\ &+ \delta(\mathbf{k} - \mathbf{Q})Nm^2, \end{aligned} \quad (32)$$

where the term which diverges at $\mathbf{k} = \mathbf{Q}$ arises from separable cluster diagrams in which the two external points are disconnected from each other and both are separability points. One can easily verify that the reducibility properties discussed in Ref. 25 do not apply here at $\mathbf{k} = \mathbf{Q}$, because of the spin operator $\sigma_z(i)$ for each external point. The resulting expression is constituted by the product of the two identical vertex corrections one for each external point and is given by m which coincides with the staggered magnetization discussed in the next subsection.

2.2 The FHNC scheme for $n(\mathbf{r}_{ij})$

The one-body density matrix is defined as

$$n(\mathbf{r}_{11'}) = \sum_\sigma \xi^*_\sigma(1')\hat{n}(1,1')\xi_\sigma(1), \quad (33)$$

$$\hat{n}(11') = \frac{A}{\aleph} \sum_{r_2 \ldots r_A, \sigma_2 \ldots \sigma_A} \Phi^*_{SDW}(12..A) \prod_{i,j \neq 1,1'} f(r_{1'i}) f(r_{ij}) \times \prod_{i<j \neq 1,1'} f^2(r_{ij}) \Phi_{SDW}(1'2...A). \quad (34)$$

If the correlation $f(r_{ij})$ is set equal to 1, the uncorrelated one-body density matrix $n(r_{11'}) = l_u(r_{11'})$. More generally, the one-body density matrix is the u component of $\hat{n}(1,1')$. Its cluster expansion can be easily deduced from that given in Ref. 26 for a continuous system, following the procedure outlined in the previous subsection for $g(r_{ij})$. One ends up with the result

$$n(11') = \sum_p \rho^p \sum_{r_2,\ldots,r_p} \hat{L}_p(1,1',r_3,\ldots,r_p), \quad (35)$$

where $\hat{L}_p(1,1',r_3,\ldots,r_P)$ is the sum of the linked, topologically distinct terms having two external indices (1 and 1') and $p-1$ internal indices. Each term is a product of dynamical and statistical correlations. The dynamical correlations having 1 or 1' as particle variable must be of the type $\xi(r) = f(r) - 1$. As discussed in Ref. 26, the reducibilities in 1 and 1' cannot be removed and they appear as vertex corrections. The density matrix is given by:

$$\hat{n}(11') = n_0\{\hat{\rho}(11') - 2\hat{N}_{\xi c \xi c}(11') - 2\hat{E}_{\xi c \xi c}(11')\} \exp\{N_{\xi\xi}(r_{11'}) + E_{\xi\xi}(r_{11'})\}. \quad (36)$$

The FHNC equations for the vertex correction n_0, the chain functions $N_{\xi\xi}$, $N_{\xi d}$, $N_{\xi e}$ and the composite functions $X_{\xi\xi}$, $X_{\xi d}$, $X_{\xi e}$ coincide with those of the paramagnetic case[13] and will not be reported here. To calculate the chain-operator $\hat{N}_{\xi c \xi c}$,one has first to evaluate the chain operator $\hat{N}_{\rho\alpha}(1,i)$ having ρ as the first element of the chain (that having 1 as particle variable) which is $\hat{\rho}$, provided by the integral equation:

$$\hat{N}_{\rho\alpha}(1,i) = -\frac{1}{2}\hat{\rho}(1,i) + (\hat{N}_{\rho\alpha}(1,k)|\hat{X}_{cc}(k,i) - \frac{1}{2}(\hat{X}_{cc}(k,l)|\hat{\rho}(l,i))), \quad (37)$$

and the chain operator $\hat{N}_{X\alpha}(1,i)$ having $\hat{X}_{\xi c}$ as first element:

$$\hat{N}_{X\alpha}(1,i) = \hat{X}_{\xi c}(1,i) - \frac{1}{2}(\hat{X}_{\xi c}(1,k)|\hat{\rho}(k,i)) + (\hat{N}_{X\alpha}(1,k)|\hat{X}_{cc}(k,i) - \frac{1}{2}(\hat{X}_{cc}(k,l)|\hat{\rho}(l,i))). \quad (38)$$

The chain operator $\hat{N}_{\xi c \xi c}(1,1')$ is given by:

$$\hat{N}_{\xi c \xi c}(1,1') - \frac{1}{2}\hat{\rho}(1,1') = (\hat{N}_{\rho\alpha}(1,i)|\hat{X}_{c\xi}(i,1')) + (\hat{X}_{\xi c}(1,i)|\hat{N}_{\alpha\rho}(i,1')) + (\hat{N}_{X\alpha}(1,i)|\hat{X}_{\alpha\xi}(i,1')) + \hat{N}_{\rho\alpha}(1,1') - (\hat{N}_{\rho\alpha}(1,i)|\hat{X}_{\alpha c}(i,1')), \quad (39)$$

where

$$\hat{X}_{\xi c}(1,i) = (g_{\xi c}(r_{1i}) - 1)(\hat{N}_{\xi c}(1,i) - \frac{1}{2}\hat{\rho}(1,i)) + g_{\xi d}(r_{1i})\hat{E}_{\xi c}(1,i), \quad (40)$$

$$\hat{N}_{\xi c}(1,i) = (\hat{X}_{\xi c}(1,k) + \hat{N}_{\xi\alpha}(1,k) - \frac{1}{2}\hat{\rho}(1,k)|\hat{X}_{cc}(k,i) - \frac{1}{2}(\hat{X}_{cc}(k,l)|\hat{\rho}(l,i))) - \frac{1}{2}(\hat{X}_{\xi c}(1,k)|\hat{\rho}(k,i)). \quad (41)$$

The staggered magnetization m is defined as

$$m = \frac{1}{N} < S^z_{\mathbf{Q}} > = < \sum_{\mathbf{k}} c^\dagger_{\mathbf{k}+\mathbf{Q},\alpha} \sigma^z_{\alpha,\alpha'} c_{\mathbf{k},\alpha'} > . \quad (42)$$

It is related to $\hat{n}(11')$ by the equation

$$m = \frac{1}{N} \sum_{r_1} e^{i\mathbf{Q}\cdot r_1} (n_\uparrow(r_{11'} = 0) - n_\downarrow(r_{11'} = 0)), \quad (43)$$

where $n_\sigma(r_{11'}) = \xi^*_\sigma(1')n(1,1')\xi_\sigma(1)$. In the case of ordinary paramagnetic wave function $m = 0$ since $n_\uparrow = n_\downarrow$.

The u-part of $n(1,1')$ does not contribute, because it does not depend upon σ. One gets the result

$$m = 2n_u(r_{11'} = 0). \quad (44)$$

For the uncorrelated model, $n_u(0) = l_u(0)$ and one recovers eq. (9).

2.3 Excitation spectrum

As in the case of the paramagnetic model[13,27], the single particle excitation spectrum $e(\mathbf{p})$ can be calculated by modifying $\hat{\rho}(1,2)$:

$$\hat{\rho}_p(1,2) = \hat{\rho}(1,2) + \alpha \hat{f}_p(1,2), \quad (45)$$

where

$$f_p^u(\mathbf{r}_{12}) = \frac{1}{2}\sum_{\mathbf{p}_i\in S_p}[v^2(\mathbf{p}_i)\cos(\mathbf{p}_i\cdot\mathbf{r}_{12}) + u^2(\mathbf{p}_i)\cos((\mathbf{p}_i+\mathbf{Q})\cdot\mathbf{r}_{12})] - \frac{1}{2}\sum_{\mathbf{k}_i\in S_p}[u^2(\mathbf{k}_i)\cos(\mathbf{k}_i\cdot\mathbf{r}_{12}) - v^2(\mathbf{k}_i)\cos((\mathbf{k}_i+\mathbf{Q})\cdot\mathbf{r}_{12})], \quad (46)$$

$$f_p^v(\mathbf{r}_{12}) = -\frac{1}{2}\sum_{\mathbf{p}_i\in S_p}u(\mathbf{p}_i)v(\mathbf{p}_i)[\cos(\mathbf{p}_i\cdot\mathbf{r}_{12}) + \cos((\mathbf{p}_i+\mathbf{Q})\cdot\mathbf{r}_{12})] + \frac{1}{2}\sum_{\mathbf{k}_i\in S_p}u(\mathbf{k}_i)v(\mathbf{k}_i)[\cos(\mathbf{k}_i\cdot\mathbf{r}_{12}) + \cos((\mathbf{k}_i+\mathbf{Q})\cdot\mathbf{r}_{12})], \quad (47)$$

where S_p is the set of momenta $\mathbf{k}_i$ characterizing the shell p. The terms linear in α in the expression $E_0(\hat{\rho}_p) - E_0(\hat{\rho})$, give $e_0(p) - e_0(k_F)$. A similar procedure can be used to evaluate the hole energies $e(h)$. The quantities $f^u_{k_F}$ and $f^v_{k_F}$ are different from zero, which implies the presence of a gap. It is easy to verify that, in the uncorrelated case, the above method leads to eq. (8).

The particle-hole correlated states Ψ_{ph} are not orthogonal to each other. However, it has been proved that, in the calculation of the diagonal matrix elements, the orthogonality corrections vanish in thermodynamic limit.

The behavior of the CBF theory based on $np-nh$ SDW-states as a function of the coupling constant U/t is an interesting issue. Particularly, in the limiting case, $U/t\to\infty$ and $\nu=\frac{1}{2}$ the uncorrelated energy is already the best upperbound, therefore $f=1$ and the *variational* single particle spectrum is given by $e_0(k)$ of eq. (8) which diverges. In fact, in this critical case, the number of states providing a finite energy expectation value is given by the square root of that allowed at any other finite value of U/t. As a consequence there are many states of the $np-nh$ basis which lead to unphysical energy expectation values. The understanding of the interplay between the $np-nh$ states and the magnon states[14] generated by the spin density fluctuation operator $\rho_{\sigma,k}$ could be relevant for this problem. Work in this direction is in progress.

3 Results and discussion

In this section, we review some numerical results obtained[13,29] for the $1D$ Hubbard model and present some preliminary results for the $2D$-SQL case[30].

The convergence of the FHNC scheme with respect to the inclusion of bridge diagrams has been studied for the $1D$-Gutzwiller ansatz

$$G_J = \prod_{i<j} f_\sigma(\mathbf{r}_{ij}) = \prod_{i<j}(1-(1-g)\delta_{r_i,r_j,1}), \quad (48)$$

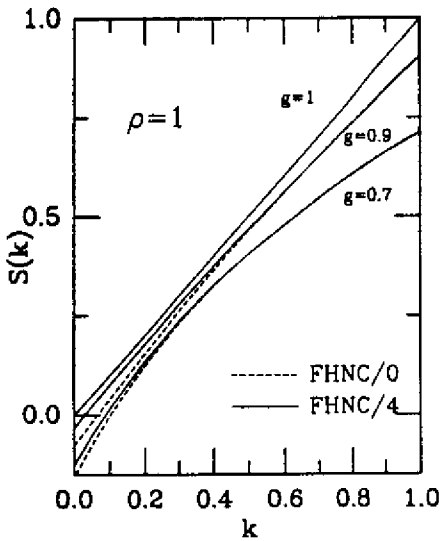

Fig.2 Taken from Ref. 13. $1D$-Hubbard model, $U/t=4$. Density-density correlation functions for the Gutzwiller paramagnetic ansatz at $\rho=1$. Solid and dashed lines correspond to calculations using FHNC/4 and FHNC/0, respectively. Results for values $g=0.7$ and 0.9 of the variational parameter are compared with the Hartree-Fock ($g=1$) results. k is in units of π/a.

and the paramagnetic Slater determinant Φ_p, for which case exact results are available[31]. It has been found that FHNC/0 (no bridge diagrams) already provides an estimate of E/Nt for $U/t\le 4$ and $\rho=1$ which is accurate within less

Table I Total energy E/Nt of the $1D$-Hubbard hamiltonian with $U/4t = 1$ calculated for various variational paramagnetic models, by using FHNC/4 (FHNC) or second order Power Series[28,13] (PS) approximation, and compared with the exact Gutzwiller model[31] (G_{exact}) and the exact results by Lieb and Wu[8]. G, J, S, Q stand for Gutzwiller, Jastrow, Gutzwiller-spin, Gutzwiller-quartet paramagnetic models, respectively. The bottom row displays the results of the one-body density matrix for the G-model at $r = 0$, calculated in FHNC/4 approximation.

ρ	1	0.8	0.6
G_{exact}	−0.518	−0.764	−0.791
$EXACT$	−0.573	−0.788	−0.821
G_{FHNC}	−0.519	−0.763	−0.792
J_{FHNC}	−0.520	/	/
J_{PS}	−0.522	/	/
S_{PS}	−0.528	/	/
Q_{FHNC}	−0.560	−0.779	−0.819
$n_{FHNC}(0)$	0.99	0.79	0.60

than 10%. The accuracy is somewhat worse for the sum rules $S(0) = S_\sigma(0) = 0$ and $n(0) = \rho$. The FHNC/4 approximation improves the results of E/Nt which are in agreement with the corresponding exact values for $U/t \leq 10$ at all values of ρ. For larger values of the coupling constant and, consequently smaller values of g ($g \leq 0.4$), the FHNC scheme has a low convergence and one needs to go beyond FHNC/4.

Typical results of the density-density correlation function $S(k)$ are displayed in Fig.2 for $\rho = 1$. The effect of correlation is quite large even at $g = 0.9$. The contribution of bridge diagrams increases for larger values of the filling factor and smaller values of g. Their effect becomes negligible for $|\mathbf{k}| \geq \frac{1}{2}k_F$. $S(0)$ can be forced to be zero by redefining $S(k)$ in a small region of k around zero[32], with

practically no change in E/Nt.

The results for E/Nt and $n(0)$ are summarized in Table I at $U/t = 4$. The second row of the Table displays the exact results for the $1D$-Hubbard hamiltonian by Lieb and Wu while the second row from the bottom shows the FHNC/4

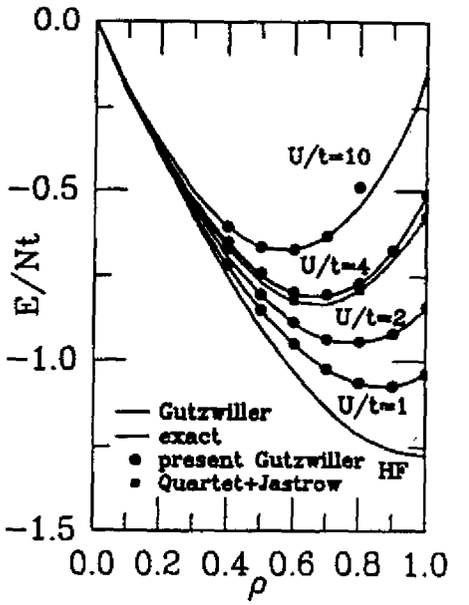

Fig.3 Taken from Ref. 13. The total energy for the $1D$ Hubbard model.The results obtained for the Gutzwiller paramagnetic wave function in FHNC/4 approximation are compared with the exact Gutzwiller results[31]. At $U/t = 4$, the estimates of the Quartet+Gutzwiller model which includes $e - d$ correlation are compared with the exact results of Lieb and Wu[8].

results[13] for a correlation operator which includes four-particle correlations (quartets):

$$G = G_G \prod_{i<j<k<l} f^{(4)}(i,j,k,l), \tag{49}$$

$$f^{(4)}(i,j,k,l) = \begin{cases} \eta & \text{if } r_{ij}=0, |r_{ik}|=a, |r_{il}|=2a, |r_{kl}|=3a, \\ 1 & \text{otherwise.} \end{cases} \quad (50)$$

The quartet-correlations simulate short-range $e-d$ correlations, discussed originally by Kaplan, Horsch and Fulde[18] and later by others[18,33]. The estimate of E/Nt as a function of ρ at various values of $U/4t$ are shown in Fig. 3 and the resulting momentum distribution is displayed in Fig. 4. The following comments are in oder:

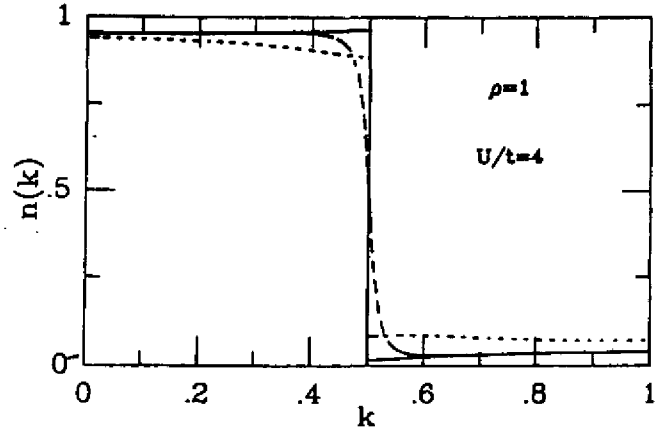

Fig.4 Momentum distribution functions for different correlated $1D$-models at $U/t = 4$ and $\rho = 1$. The $n(k)$ of the two paramagnetic wavefunctions ($\Delta = 0$) (solid: Gutzwiller; short-dashes: $e-d$) show the effect of quartet-correlations. The antiferromagnetic wave function (long-dashes) has $\Delta = 0.48$ and $g = 0.5$.

(i) FHNC/0 and FHNC/4 approximations look reasonable for moderate values of the coupling constant ($U/t \leq 4$ for FHNC/0 and $U/t \leq 10$ for FHNC/4). The accuracy is expected to improve in more than one dimensional models; (ii) nearest-neighbor scalar ((J) in Table I) or spin-dependent ((S) in Table I) correlations do not lead to a significant lowering of the energy upperbound in the $1D$ paramagnetic case[13]; (iii)the quartet correlations account for 90% of the discrepancy between the results of the Gutzwiller model and the exact

eigenfunctions[13,15]; (iv) the quartet correlations lead to a decrease of $n(k)$ for $k \leq k_F$, in accordance with the exact solution by Lieb and Wu; (v) the correlated paramagnetic wave function bear the Fermi liquid character which, strictly speaking, is incorrect at least in $1D$[34,7]; in spite of this, the energy upperbounds in the quartet-Gutzwiller model are very close to the exact results.

On the contrary, the correlated BCS[13,35] or the correlated SDW lead to a $n(k)$ which is continuous across k_F. In the following we discuss some preliminary results[29,30] obtained for the Jastrow correlated SDW wavefunction.

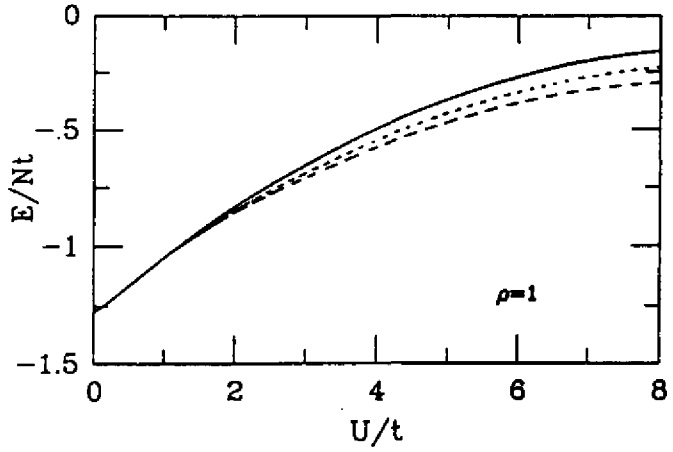

Fig.5 Energy expectation values of the $1D$-Hubbard model as a function of U/t. The results of the Gutzwiller correlated paramagnetic modal [13,12] (solid line) and those of Gutzwiller correlated SDW model (short dashes)[29,12] are compared with the exact solution (long dashes)[8].

The $1D$-model results for momentum distribution and the energy upperbound are given in Figs. 4 and 5. The AF model is energetically preferred with respect to the paramagnetic one at all values of the coupling constant U/t. The FHNC/0 results agree with those of Ref. 12 within less than 5%. The smallest value of g occurs at $U/t = 4$ ($g = 0.6$) with $g = 1$ at both $U/t = 0$ and

∞. FHNC/4 is expected to reproduce the Monte Carlo results. The momentum distribution of the AF wave function differs from that of the paramagnetic one, mainly because of its continuous behavior across k_F. The features due to $e-d$ correlations, shown in Fig. 4, are not reproduced by the SDW correlations, which strongly indicates that $e-d$ correlations are important for the SDW model, too.

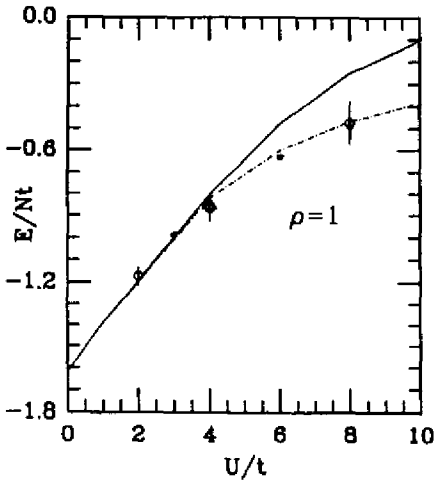

Fig.6 Energy expectation values of the $2D$-SQL model as a function of U/t. The results of the Gutzwiller correlated paramagnetic model (solid line) and SDW (dot-dashed line) models are compared with Hirsch's QMC results[9] (open circle and bars), that of Parola *et al.*[34] (triangle). and those of Yokoyama and Shiba[12] (*solid square*)

Preliminary results[30] obtained for the $2D$-SQL model at half filling are given in Figs. $6-8$. As in the one dimensional case, the AF model is variationally prefered with respect to the paramagnetic one. The FHNC/0 evaluations are in good agreement with the Monte Carlo estimates of Ref. 12. For instance at $U/t=4$ variational Monte Carlo gets $E/Nt=-0.84$ with $g=0.65$, $\Delta=0.45$ and $m=0.58$ which compares reasonably well with the FHNC/0 results reported in Fig. 6 and Table II. In Fig. 6 the QMC estimates[9], the variational MC

calculation[12] and the results of 4×4 exact diagonalization[34] are reported for comparison.

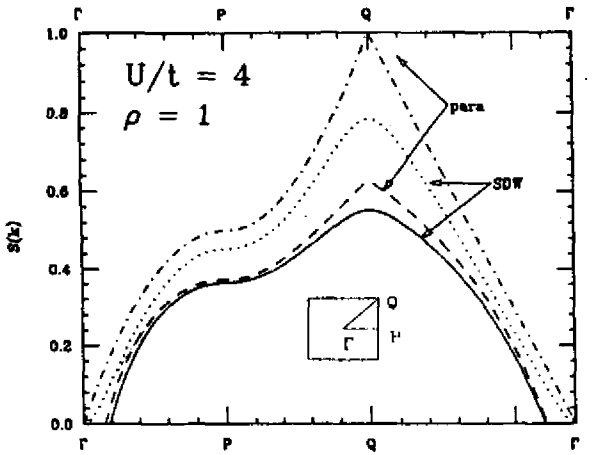

Fig.7 Density-density correlation functions $S(\mathbf{k})$ for the Gutzwiller correlated paramagnetic and AF models for the $2D$-SQL Hubbard hamiltonian at $\rho=1$ and $U/t=4$. The dotted and dot-dashed curves report the uncorrelated $S_{un}(\mathbf{k})$. All the results displayed, correspond to wave functions having the *optimal* values for the variational parameters g and Δ.

The density-density correlation function $S(\mathbf{k})$ and the momentum distribution $n(\mathbf{k})$ are plotted in Figs. 7, 8 by following the path $\Gamma PQ\Gamma$ displayed in the insert Fig. 7. The correlated $S(\mathbf{k})$ should, in fact, heal to zero at Γ ($S(0)=0$). The failure of this sum rule is entirely due to the lackness of elementary diagrams in FHNC/0 approximation. FHNC/4 approximation leads[30] indeed to a much better fulfillment of the sum rule, although the energy estimates change very little. Some preliminary results obtained away from half filling ($\rho=0.95$ and $\rho=0.90$) are reported in Table II. They show that the Gutzwiller correlated models lead to AF-LRO away from half filling. Such interesting result persists in the Jastrow model, too[30], and it is in agreement with the 4×4 exact diagonalization calculation of Ref. 34.

Table II. Breakdown of the energy and the staggered magnetisation for the Gutzwiller correlated $2D$-SQL model calculated in FHNC/0 approximation.

ρ	1.0	1.0	1.0	0.946	0.946	0.90	0.90
U/t	1.0	4.0	6.0	1.0	4.0	4.0	6.0
g	0.85	0.62	0.98	0.86	0.60	0.61	0.50
Δ	0.02	0.43	2.40	0.02	0.30	0.06	0.39
$< T >$	-0.60	-1.48	-1.10	-1.61	-1.48	-1.49	-1.38
$< V >$	0.21	0.66	0.50	0.20	0.57	0.50	0.62
E/Nt	-1.39	-0.82	-0.60	-1.41	-0.91	-0.99	-0.76
m	0.20	0.41	0.81	0.02	0.30	0.08	0.34
$S(\pi,\pi)$	0.78	0.54	0.21	0.91	0.60	0.64	0.49
$S_\sigma(\pi,\pi) - m^2N$	1.19	1.21	0.25	1.11	1.34	1.46	1.19

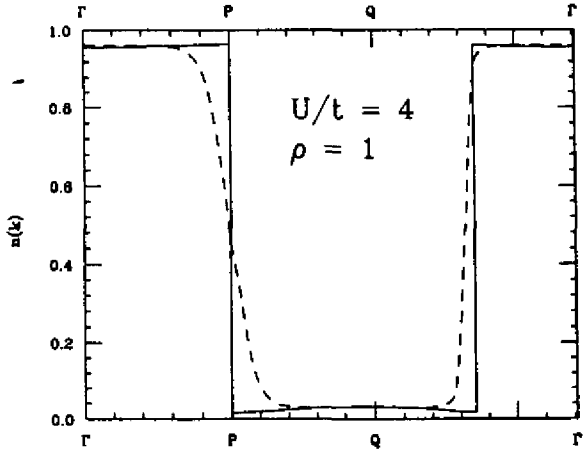

Fig.8 Momentum distribution of the Gutzwiller-correlated $2D$-SQL Hubbard model. The solid curve refers to the paramagnetic wave function and the dashed curve to the SDW wave function.

For a more realistic evaluation of the $U/t - \rho$ phase diagram, it is necessary to go beyond the Jastrow-type correlation operator. This can be done either by including triplet and quartet correlations in G or by employing CBF theory. Work in this direction is in progress.

References

[1] M.H.Kalos, *Phys. Rev.* **A2**, 250(1970); D.M.Ceperley and M.H. Kalos, in *Monte Carlo Method in Statistical Physics*, K. Binder ed. (Springer, Berlin 1978).

[2] E. Feenberg, *Theory of Quantum Liquids*, (Academic Press, New York 1969)

[3] *Recent Progress in Many-Body Theory*, Vol.I , A. Kallio, E. Pajanne and R. F. Bishop, eds., (Plenum Press, London, 1981).

[4] J. Hubbard, *Proc. Roy. Soc.* **A276**, 238(1964); **A285**, 542(1965).

[5] D. Vollhardt, *Rev. Mod. Phys.* **56**, 99(1984).

[6] W. F. Brinkman and T. M. Rice, *Phys. Rev.* **B 2**, 4302(1970).

[7] P. W. Anderson, *Science* **235**, 1196 (1987).

[8] E. H. Lieb and F. Y. Wu, *Phys. Rev. Lett.* **20**, 1445 (1968).

[9] J.E. Hirsch, *Phys. Rev.* **B31**, 4403 (1985); J.E. Hirsch and H.Q. Lin, *Phys. Rev. Lett.* **31**, 4403 (1989).

[10] S. Sorella, E. Tosatti, S. Baroni, R.Car, and M. Parrinello, *Intern. J. Mod. Phys.* **B1**, 993 (1988); S. Sorella, S. Baroni, R.Car, and M. Parrinello, *Europhys. Lett.* **8**, 663 (1989).

[11] C. Gros, R.Joynt, and T.M. Rice, *Phys. Rev.* **B36**, 381 (1987).

[12] H. Yokoyama and H. Shiba, *J. Phys. Soc. Jap.* **56**, 1490, 3570, 3582 (1987).

[13] S. Fantoni, X.Q. Wang, E. Tosatti, and Lu Yu, *Physica* **C153**, 1255 (1988); S. Fantoni, X.Q. Wang, E. Tosatti, Lu Yu and M. Viviani, submitted to *Phys. Rev.* **B**.

[14] E. Manousakis, Tallohssee preprint (1989) and references therein.

[15] T. A. Kaplan, P. Horsch and P. Fulde, *Phys. Rev. Lett.* **49**, 889(1982). P. Fazekas and K. Penc, *Int. J. Mod. Phys.* **B1** 1021(1988)

[16] E. Krotscheck, R. A. Smith, J. W. Clark and R. M. Panhoff, *Phys. Rev.* **B 24**, 6383(1981).

[17] V.R.Pandharipande and R.B. Wiringa, *Rev. Mod. Phys.* **51**, 821 (1979).

[18] M. Viviani, A. Buendia, S. Fantoni, and S. Rosati, *Phys. Rev.* **B 38**, 4523(1988).

[19] T. M. Rice, contribution in this volume.

[20] J. W. Clark, L. R. Mead, E. Krotscheck, K. E. Kurten and M.L. Ristig, *Nucl. Phys.* **A328**, 45(1979); E. Krotscheck and R. A. Smith, *Phys. Rev.* **B27**, 4222(1983); J. W. Clark, in *Progress in Particle and Nuclear Physics*, ed. D.H. Wilkinson (Pergamon, Oxford, 1979), Vol. 2.

[21] S. Fantoni, B.Friedman, and V. R. Pandharipande, *Nucl. Phys.* **A386**, 1(1982); **A339**, 1(1983); A. Fabrocini and S. Fantoni, *First Int. Course on Condensed Matter*, ACIF series Vol. 8, eds. D. Prosperi, S. Rosati, and G. Violini, eds. (World Sci., Singapore, 1986) and references therein.

[22] J. R. Schrieffer, X. G. Wen and S. C. Zhang, *Phys. Rev.* **B39**, 11663(1989).

[23] G. Shirane *et al. Phys. Rev. Lett.* **59**, 1613(1987). J. Tranrquada *et al. Phys. Rev. Lett* **60**, 156(1988).

[24] K. B. Lyons *et al. Phys. Rev.* **B37**, 2353(1988); *Phys. Rev. Lett* **60**, 732(1988).

[25] S. Fantoni and S. Rosati, *Nuovo Cim.* **20A**, 179 (1974); **25A**, 593(1975).

[26] S. Fantoni, *Nuovo Cim.* **44A**, 191 (1978).

[27] B. Friedman and V.R. Pandharipande, *Phys. Lett.* **B100**, 205 (1981).

[28] S. Fantoni and V. R. Pandharipande, *Phys. Rev.* **C37**, 1697 (1988).

[29] X. Q. Wang, S. Fantoni, E. Tosatti and Lu Yu, Perceedings of *XIII* International Workshop on Condensed Matter Theories, V. C. Angnilera-Navaro *et al.*, eds., to be published by Plenum Press.

[30] X. Q. Wang *et al.*, in preparation.

[31] W. Metzner and D. Vollhardt, *Phys. Rev. Lett.* **59**, 121 (1987); F. Gebhardt and D. Vollhardt, *Phys. Rev. Lett.* **59**, 1472 (1987).

[32] E. Krotscheck, *Nucl. Phys.* **A 317**, 149 (1979).

[33] D. Baeriswyl, in *Nonlinearity of Condensed Matter Physics*, A.R.Bishop *et al.*, eds. (Springer, Berlin 1987) *p.*183.

[34] A. Parola, S. Sorella, E. Tosatti, and M. Parrinello, to be published.

[35] S. Fantoni, *Nucl. Phys.* **A 363**, 381 (1981).

Stampato in proprio nella tipografia
del Centro Internazionale di Fisica Teorica